AIP | Review of Scientific Instruments

# Tomography experiment of an integrated circuit specimen using 3MeV electrons in the transmission electron microscope

Hai-Bo Zhang, Xiang-Liang Zhang, Yong Wang, and Akio Takaoka

Citation: Rev. Sci. Instrum. **78**, 013701 (2007); doi: 10.1063/1.2409864
View online: http://dx.doi.org/10.1063/1.2409864
View Table of Contents: http://rsi.aip.org/resource/1/RSINAK/v78/i1
Published by the American Institute of Physics.

# Tomography experiment of an integrated circuit specimen using 3 MeV electrons in the transmission electron microscope

Hai-Bo Zhang,[a] Xiang-Liang Zhang, and Yong Wang
*Department of Electronic Science and Technology, Xi'an Jiaotong University, Xi'an 710049, People's Republic of China and Key Laboratory for Physical Electronics and Devices of the Ministry of Education, Xi'an Jiaotong University, Xi'an 710049, People's Republic of China*

Akio Takaoka
*Research Center for Ultrahigh-Voltage Electron Microscopy, Osaka University, Yamada-oka 2-1, Suita, Osaka 565-0871, Japan*

(Received 18 June 2006; accepted 19 November 2006; published online 4 January 2007)

The possibility of utilizing high-energy electron tomography to characterize the micron-scale three dimensional (3D) structures of integrated circuits has been demonstrated experimentally. First, electron transmission through a tilted $SiO_2$ film was measured with an ultrahigh-voltage electron microscope (ultra-HVEM) and analyzed from the point of view of elastic scattering of electrons, showing that linear attenuation of the logarithmic electron transmission still holds valid for effective specimen thicknesses up to 5 $\mu$m under 2 MV accelerating voltages. Electron tomography of a micron-order thick integrated circuit specimen including the Cu/via interconnect was then tried with 3 MeV electrons in the ultra-HVEM. Serial projection images of the specimen tilted at different angles over the range of ±90° were acquired, and 3D reconstruction was performed with the images by means of the IMOD software package. Consequently, the 3D structures of the Cu lines, via and void, were revealed by cross sections and surface rendering. © *2007 American Institute of Physics.*
[DOI: 10.1063/1.2409864]

## I. INTRODUCTION

With the rapid development of integrated circuit (IC) fabrication technology, the electron microscope has become a powerful tool to extract structural information and to carry out failure analysis for ICs.[1–3] As an analytical three dimensional (3D) approach with a higher spatial resolution than the conventional x-ray computed tomography, electron tomography (ET) is mainly based on transmission electron imaging. It came into biology researches in the 1970s,[4] and extended to materials, physical, and chemical applications in the past few years.[5–8] Nevertheless, only a very limited number of ET results obtained with the transmission electron microscope (TEM) have been reported so far for semiconductor device and IC specimens.[9–12] Moreover, the specimens in these ET experiments were relatively thin, e.g., a 0.1 $\mu$m thick barrier/seed layer stack of Cu interconnects.[11] Conversely, ICs usually possess micron-scale structures, though their lines become more and more narrow. Direct characterization of a complete large 3D structure in such IC specimens, instead of 3D reconstruction from serial thin sections, also poses a challenge to ET. This is because both the quality of transmission electron images and the linearity between the logarithmic transmission electron intensity and mass thickness may deteriorate with the increase in multiple scattering and inelastic scattering of electrons within thick specimens.[13–15]

Utilization of the ultrahigh-voltage electron microscope (ultra-HVEM) whose accelerating voltage exceeds 1 MV or the scanning transmission electron microscope (STEM) can be considered at the present time for improving image quality of thick specimens.[16–18] Here, for very thick specimens, the ultra-HVEM has a better resolution than the conventional STEM whose accelerating voltages are lower than 300 kV, for example, ~5 nm (Ref. 19) and ~80 nm,[17] respectively, for objects below a 5 $\mu$m thick amorphous layer. Although some theories of STEM tomography in the multiple-scattering regime and bright-field imaging have been proposed recently,[20,21] further experimental efforts are still needed before they are applicable to several micron thick specimens. Accordingly, the aim of the present work is to try ET of a micron-order thick IC specimen using the ultra-HVEM (Ref. 22) at Osaka University, whose highest accelerating voltage of 3 MV for TEM use is also the world's highest among all TEMs.

## II. ELECTRON TRANSMISSION

Electron transmission through a specimen is an important factor for ET because 3D reconstruction is conventionally carried out on the assumption of linearity between the logarithmic electron transmission and the mass thickness along the path of incident electrons.[23] The linearity, i.e., the exponential attenuation characteristic of electron transmission through the specimen, results from both single elastic scattering and restriction of an objective aperture used to produce amplitude contrast in TEMs.[23] However, tilting the specimen in ET increases the effective thickness of the specimen, and this may aggravate the projection linearity espe-

[a]Author to whom correspondence should be addressed; electronic mail: hbzhang@mail.xjtu.edu.cn

 

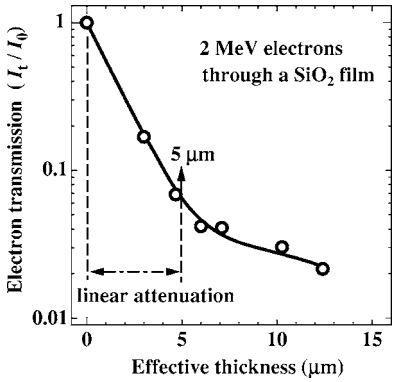


FIG. 1. Measured variation of the normalized electron transmission $I_t/I_0$ with the effective thickness of a tilted $SiO_2$ film specimen in the ultra-HVEM. Here, $I_t$ denotes the intensity of electrons collected by a Faraday cup, which pass through not only the specimen but also the objective aperture; $I_0$ is defined as the corresponding beam current at the Faraday cup without the specimen.

cially for thick specimens due to multiple elastic scattering. Therefore, we first investigate the relation between electron transmission and the effective thickness of a tilted $SiO_2$ film specimen with the ultra-HVEM. Here, the effective thickness $H$ of the specimen changes with the tilt angle $\theta$ in the form $H \approx h/\cos\theta$, where $h$ is the real thickness of the specimen and is 3 $\mu$m in our work. Tilting the specimen with a 360° tilt holder,[24] we can hence obtain variations of the electron transmission (in a logarithmic scale) with the effective thickness of the specimen, as shown in Fig. 1. Evidently, the linear attenuation characteristic of the logarithmic electron transmission holds valid for the effective thickness up to 5 $\mu$m. This thickness range should be adequate for ET of conventional thick IC specimens with the ultra-HVEM. Note that the slope of the logarithmic electron transmission in its linear attenuation range is[23]

$$-\beta = -(N_A/A)\sigma_0\rho, \tag{1}$$

where the attenuation coefficient $\beta$ is independent of the specimen thickness. Here, $N_A$ is Avogadro's number, $A$ the atomic weight of the specimen, $\sigma_0$ the partial cross section, and $\rho$ the mass density of a specimen along the path of electrons. The parameter $\sigma_0$ usually decreases with the increase of both the energy of incident electrons and the half-angle of the objective aperture. In principle, higher energies of incident electrons and greater objective apertures will lead to a milder attenuation of electron transmission and a wider linear attenuation range. However, for some metal specimens with greater partial cross sections and higher mass density, the attenuation coefficient may increase and this will result in a narrower linear attenuation range.

On the other hand, with the increase of effective thickness, a significant portion of the incident electrons may experience multiple scattering, and the linear attenuation will be no longer valid. For single scattering, the scattered electrons whose deflection angles are greater than the half-angle of the objective aperture will not be collected, but in multiple-scattering region, some of these electrons may be scattered back into the half-angle range. As a result, the deviation from the linearity will lead to a greater value of electron transmission.[21] As also seen in Fig. 1, the electron transmission through large thicknesses does not decrease so rapidly as that through the linear attenuation range. Further, the average scattering times $n$ within the range of $L$ can be estimated from the elastic mean free path λ between scattering events,[25]

$$n = L/\lambda = (N_A/A)\sigma\rho L. \tag{2}$$

Here, by the Wentzel form for the small-angle elastic scattering,[26] the scattering cross section $\sigma$ decreases with the increase of the energy of incident electrons, in an inverse proportional relation. For the $SiO_2$ film in our work, taking its density $\rho$ and the average $A$ as 2.6 g/cm$^3$ and 21.6, respectively, the elastic mean free path of 2 MV electrons is 316 nm and the resultant average scattering times within the 5 $\mu$m linear attenuation range shown in Fig. 1 is 16. Consequently, depending mainly on the electron energy and specimen properties, the linear attenuation of electron transmission takes place in the range over which single scattering or scattering at several times dominates, however difficult it is to determine the range accurately.

## III. EXPERIMENTAL METHOD

The IC specimen including Cu interconnects and the filled via between layer lines for conduction, in our ET experiment, was prepared using a focused ion beam (FIB). The rod-shaped specimen with a base was then mounted between two small clamp plates of the 360° tilt holder and could be freely tilted about an axis parallel to the $y$ axis.

A tilt series of projection images of the specimen were then collected with the ultra-HVEM working under conditions of the 3 MV accelerating voltage and 25 000 × magnification. In the experiment, by tilting the specimen at an interval of 1° over the range of ±90°, we recorded 181 images with a high-performance cooled charge-coupled-device (CCD) camera. Here, the electron beam intensity and

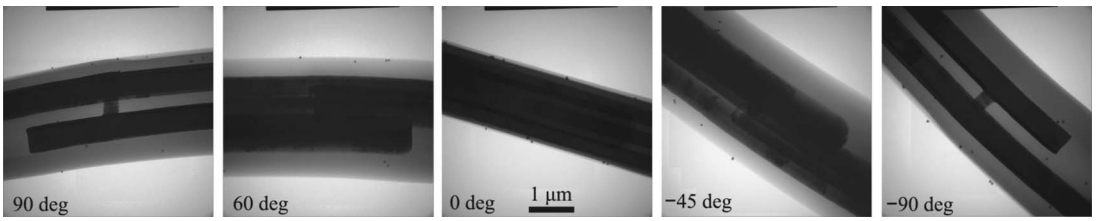


FIG. 2. Selected ultra-HVEM projection images of an IC specimen at different tilt angles, taken under conditions of the 3 MV accelerating voltage and 25 000 × magnification. The rod-shaped specimen, whose effective thickness is in the approximate range of 1.5–2.5 $\mu$m, includes the Cu interconnects and via buried in $SiO_2$ layers.

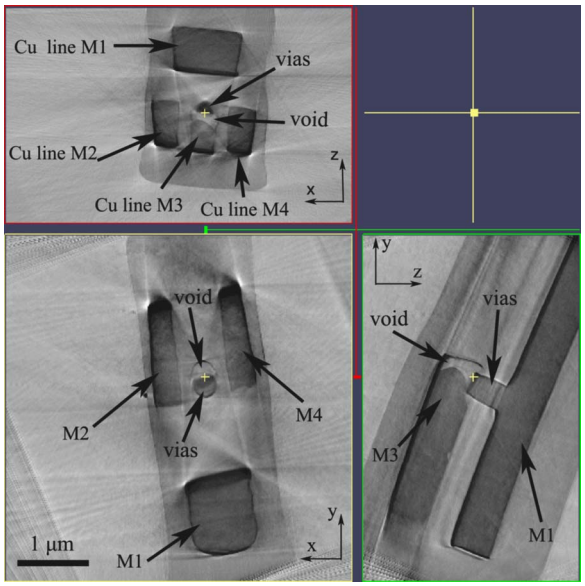


FIG. 3. (Color online) Reconstructed cross sections of the IC specimen simultaneous in three directions, perpendicular to the $y$ axis (upper left), the $z$ axis (lower left), and the $x$ axis (lower right), respectively. A thick Cu line (M1), three thin Cu lines (M2, M3, and M4), a via connecting M1 and M3, and a void appearing at the end of M3 and near the junction of the via and M3 are clearly shown through the high-energy electron tomography based on the ultra-HVEM.

the exposure time of the CCD camera were both fixed to give the same exposure amount for all images. A relatively bigger objective aperture of 50 $\mu$m was chosen to obtain more intense signals of transmission electrons for the tilted thick specimen. Figure 2 shows some ultra-HVEM images of the rod-shaped IC specimen tilted at different angles, whose effective thickness varies with the tilt angle from approximately 1.5 to 2.5 $\mu$m. The image formation here is attributed to amplitude contrast in the bright-field mode caused by the difference in mass density between Cu interconnects and $SiO_2$ layers. Moreover, high-energy electrons at 3 MeV is helpful for raising electron transmission and improving image quality by reducing chromatic aberration, though energy filtering that can further improve image quality was not employed in our ultra-HVEM. Nevertheless, 3D structural details will not be available yet from these two dimensional (2D) projections until the ET processing is completed.

Image alignment, 3D reconstruction, and result visualization in our work have been performed with the free software package IMOD (Refs. 27 and 28) developed by Colorado University especially for the ET processing of electron microscopic images on various operating systems including Linux and Windows. Here, to reduce the computation time of alignment and 3D reconstruction, margins of the ultra-HVEM projection images were wiped, and the image resolution was degraded. The image size was hence reduced from 16 bit $4096 \times 4096$ pixels to 8 bit $960 \times 960$ pixels. To raise alignment accuracy, we aligned the projection images in three steps. The cross-correlation function and the manual work were applied for the coarse alignment, and seven of the colloidal gold particles that had been deposited on the specimen were then selected as fiducial markers for the fine alignment of neighboring images. The tilt series of images were further aligned as a whole, and the logarithm was taken for image intensity. Consequently, 3D reconstruction was computed using the $R$-weighted back projection algorithm. The total computation time was about 30 min on a 2.66 GHz Pentium-4-equipped PC for the 181 projection images in this work. The obtained 3D reconstruction results can be visualized with tomographic sections, volume rendering, and surface rendering, respectively.

## IV. TOMOGRAPHIC RESULTS

Figure 3 presents the reconstructed cross sections perpendicular, respectively, to $x$, $y$, and $z$ axes, which are arranged like orthographic drawings in three directions of a 3D object. A thick Cu line (M1) and three thin Cu lines (M2, M3, and M4) are clearly shown in the xz plane (upper left) perpendicular to the $y$ axis. Moreover, a void is found to be located at the end of M3 and near the bottom of a via that connects M1 and M3. This demonstrates that the ultra-HVEM ET enables us to get 3D information of a micron-scale IC structure. Surface rendering was further implemented following surface contours of the Cu interconnects, via and void in the serial tomographic sections perpendicular to the $y$ axis. The 3D results of surface rendering in Figs. 4(a)–4(c) depict the spatial location and structure of the Cu/via interconnect and void more visually and more vividly. From Fig. 4(d) in which the Cu lines M2 and M4 are omitted, we can see again more clearly the shape of the void and its position with respect to the Cu line and the via. Note that one of the main mechanisms of void might be due to electromigration within interconnects.[29] At some high current densities, the aluminum or copper atoms in interconnects tend to migrate, leaving a void that may eventually become a discontinuity.

With regard to the ET quality actually achieved by 3D reconstruction, the accurate assessment is still a problem even now.[30] From Crowther's criterion, however, the 3D reconstruction resolution $d$ for a spherical object with the diameter $D$ from a series of $N$ projections on the specimen tilt range of ±90° can be evaluated with[23]

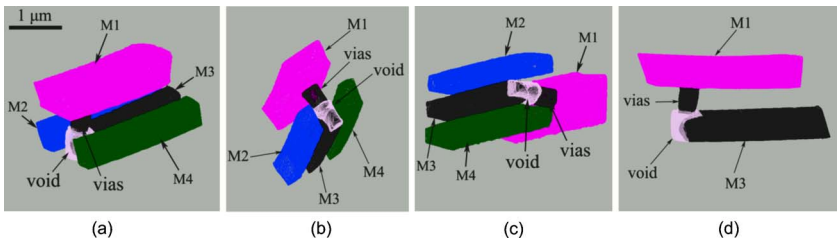


FIG. 4. (Color online) Surface rendering of 3D reconstruction results of the Cu/via interconnect and the void, obtained by following contours of regions of interest in the serial tomographic sections perpendicular to the $y$ axis. [(a)–(c)] Overall view in different directions. (d) Partial view without the Cu lines M2 and M4.

$$d = \pi D/N. \quad (3)$$

Applying the criterion to our experiment can give an overall resolution of about 44 nm with $D=2.5$ $\mu$m and $N=180$. Another limitation on the ET resolution is the resolution of 2D projection images, ~5 nm from the ultra-HVEM instrumentation and ~10 nm/pixel from the CCD images finally used for 3D reconstruction, respectively, in our work.

## V. DISCUSSION

The ultra-HVEM ET appears to be a promising approach for 3D analysis of thick specimens. Incident high-energy electrons can penetrate thicker specimens with less scattering. This may raise the imaging quality in TEMs through increasing electron transmission and reducing beam broadening. Moreover, for the IC specimens including large complex structures, e.g., via and void, the TEM ET is capable of yielding the useful 3D information that is difficult for us to observe directly with the conventional 2D images of TEMs, STEMs, and scanning electron microscopes. On the other side, it had been argued that applications of ET based on the TEM bright-field imaging to IC specimens would be limited by diffraction contrast from crystalline materials.[7,10] However, we did not observe apparent diffraction contrast of the crystalline interconnects in our experiment and reconstruction results, consistent with the report[18] by Levine *et al.* This may be because crystal grains of the metals are much smaller compared with the observed IC structure and their diffraction effect can be reduced[31] in the 3D reconstruction process from many projections obtained at different tilted angles of the specimen.

Finally, it is worthy to note that the small bright regions at the partial edge of the Cu lines M2 and M4, and some radial lines, both shown in Fig. 3, should be caused by the fiducial gold particles and the 3D reconstruction error, respectively. Further work, e.g., taking some high-accuracy iterative algorithms such as the sequential iterative reconstruction technique (SIRT), seems to be required to minimize these negative effects on ET results.

## ACKNOWLEDGMENTS

This work was supported by the National Natural Science Foundation of China (Grant No. 60476018) and by the Nanotechnology Support Project of the Ministry of Education, Culture, Sports, Science and Technology (MEXT), Japan, at the Research Center for Ultra-HVEM, Osaka University. One of the authors (H.-B. Z.) is grateful to his former student Xiao-Song Qing who contributed to the initial use of IMOD.

[1] Y. Mitsui, F. Yano, H. Kakibayashi, H. Shichi, and T. Aoyama, Microelectron. Reliab. **41**, 1171 (2001).
[2] H. Zhang, Micron **33**, 515 (2002).
[3] D. P. Vallett, IEEE Trans. Nanotechnol. **1**, 117 (2002).
[4] W. Hoppe, J. Gassmann, N. Hunsmann, H. J. Schramm, and M. Sturm, Hoppe Seyler's Z. Physiol. Chem. **355**, 1483 (1974).
[5] A. J. Koster, U. Ziese, A. J. Verkleij, A. H. Janssen, and K. P. de Jong, J. Phys. Chem. B **104**, 9368 (2000).
[6] M. Koguchi, H. Kakibayashi, R. Tsuneta, M. Yamaoka, T. Niino, N. Tanaka, K. Kase, and M. Iwaki, J. Electron Microsc. **50**, 235 (2001).
[7] P. A. Midgley and M. Weyland, Ultramicroscopy **96**, 413 (2003).
[8] J. M. Thomas, P. A. Midgley, T. J. V. Yates, J. S. Barnard, R. Raja, I. Arslan, and M. Weyland, Angew. Chem., Int. Ed. **43**, 6745 (2004).
[9] E. Bugiel, I. Daberkow, M. Schatz, and H. R. Tietz, in *Proceedings of the 15th International Congress on Electron Microscopy* (Microscopy Society of Southern Africa, Durban, 2002), Vol. 3, pp. 373–374.
[10] C. Kübel, D. Hubert, W. F. Voorhout, and M. T. Otten, Microsc. Microanal. **8**, 1104 (2002).
[11] H. Stegmann, H.-J. Engelmann, and E. Zschech, Microelectron. Eng. **65**, 171 (2003).
[12] K. van Benthem *et al.*, Appl. Phys. Lett. **87**, 034104 (2005).
[13] J. Frank, B. F. McEwen, M. Radermacher, J. N. Turner, and C. L. Rieder, J. Electron Microsc. Tech. **6**, 193 (1987).
[14] H. B. Zhang, C. Yang, and A. Takaoka, J. Electron Microsc. **53**, 617 (2004).
[15] Z. H. Levine, Proc. SPIE **5674**, 1 (2005).
[16] B. F. McEwen and A. B. Heagle, Int. J. Imaging Syst. Technol. **11**, 12 (1997).
[17] S. P. Frigo, Z. H. Levine, and N. J. Zaluzec, Appl. Phys. Lett. **81**, 2112 (2002).
[18] Z. H. Levine, J. J. Gao, S. Neogi, T. M. Levin, J. H. Scott, and S. Grantham, J. Appl. Phys. **93**, 2193 (2003).
[19] H. B. Zhang, C. Yang, J. J. Li, and A. Takaoka, Rev. Sci. Instrum. **76**, 056106 (2005).
[20] Z. H. Levine, Appl. Phys. Lett. **82**, 3943 (2003).
[21] Z. H. Levine, J. Appl. Phys. **97**, 033101 (2005).
[22] A. Takaoka, K. Ura, H. Mori, T. Katsuta, I. Matsui, and S. Hayashi, J. Electron Microsc. **46**, 447 (1997).
[23] *Electron Tomography*, edited by J. Frank (Plenum, New York, 1992).
[24] H. B. Zhang, A. Takaoka, and K. Miyauchi, Rev. Sci. Instrum. **69**, 4008 (1998).
[25] D. C. Joy, *Monte Carlo Modeling for Electron Microscopy and Microanalysis* (Oxford, New York, 1995).
[26] L. Reimer, *Transmission Electron Microscopy* (Springer, Berlin, 1993).
[27] J. R. Kremer, D. N. Mastronarde, and J. R. McIntosh, J. Struct. Biol. **116**, 71 (1996).
[28] http://bio3d.colorado.edu/imod/doc/tomoguide.html
[29] See, for example, K. N. Tu, J. Appl. Phys. **94**, 5451 (2003).
[30] M. Unser, C. O. S. Sorzano, P. Thevenaz, S. Jonic, C. El-Bez, S. De Carlo, J. F. Conway, and B. L. Trus, J. Struct. Biol. **149**, 243 (2005).
[31] R. J. Feng, T. Watanabe, and A. Takaoka, *Proceedings of the 16th International Microscopy Congress* (Publication Committee of IMC16, Sapporo, 2006), p. 698.